A comparison of PM exposure related to emission hotspots in a hot and humid urban environment: Concentrations, compositions, respiratory deposition, and potential health risks

Siming You[a†], Zhiyi Yao[b†], Yanjun Dai[c], Chi-Hwa Wang[b*]

[a]NUS Environmental Research Institute, National University of Singapore, 1 Create Way, Create Tower, #15-02, Singapore 138602

[b]Department of Chemical and Biomolecular Engineering, National University of Singapore, 4 Engineering Drive 4, Singapore 117585

[c]School of Mechanical Engineering, Shanghai Jiao Tong University, 800 Dong Chuan Road, Shanghai, 200240

† Authors contribute equally to this work.

Submitted to

Science of the Total Environment

April 2017

*Corresponding Author. Tel: +65 65165079; Fax: +65 67791936;

Email: chewch@nus.edu.sg (C. H. Wang)

Abstract

Particle number concentration, particle size distribution, and size-dependent chemical compositions were measured at a bus stop, alongside a high way, and at an industrial site in a tropical city. It was found that the industry case had 4.93×10^{7} - 7.23×10^{7} and 3.44×10^{4} - 3.69×10^{4} #/m^{3} higher concentration of particles than the bus stop and highway cases in the range of 0.25-0.65 μm and 2.5-32 μm, respectively, while the highway case had 6.01×10^{5} and 1.86×10^{3} #/m^{3} higher concentration of particles than the bus stop case in the range of 0.5-1.0 μm and 5.0-32 μm, respectively. Al, Fe, Na, and Zn were the most abundant particulate inorganic elements for the traffic-related cases, while Zn, Mn, Fe, and Pb were abundant for the industry case. Existing respiratory deposition models were employed to analyze particle and element deposition distributions in the human respiratory system with respect to some potential exposure scenarios related to bus stop, highway, and industry, respectively. It was shown that particles of 0-0.25 μm and 2.5-10.0 μm accounted for around 74%, 74%, and 70% of the particles penetrating into the lung region, respectively. The respiratory deposition rates of Cr and Ni were 170 and 220 ng/day, and 55 and 140 ng/day for the highway and industry scenarios, respectively. Health risk assessment was conducted following the US EPA supplemented guidance to estimate the risk of inhalation exposure to the selected elements (i.e. Cr, Mn, Ni, Pb, Se, and Zn) for the three scenarios. It was suggested that Cr poses a potential carcinogenic risk with the excess lifetime cancer risk (ELCR) of $2.1\text{-}98\times10^{-5}$ for the scenarios. Mn poses a potential non-carcinogenic risk in the industry scenario with the hazard quotient (HQ) of 0.98. Both Ni and Mn may pose potential non-carcinogenic risk for people who are involved with all the three exposure scenarios.

Keywords

Air quality; Chemical composition; Particle number concentration; Particle size distribution; Traffic and industry.

1 Introduction

Airborne particulate matter (PM) poses a potential threat to the health of human beings via inhalation exposure. It has been widely recognized that PM exposure is associated with the increased occurrence of various diseases such as cardiovascular diseases (Donaldson et al., 2001; Liao et al., 1999), respiratory diseases (Atkinson et al., 2001; You et al., 2016), asthma (Norris et al., 1999; Tecer et al., 2008), and lung cancer (Turner et al., 2011). Although the fundamental mechanisms governing the harmful effects on human health are still not fully understood, it is generally recognized that particle number or mass concentration, particle sizes, and size-dependent chemical composition are critical factors affecting human inhalation exposure (Nel, 2005). The size of airborne particles not only affects the amount of particles inhaled but also the distribution of inhaled particles in the human respiratory system. Generally, compared to microparticles, nanoparticles have a greater ability to penetrate deeply into the alveolar region and coat airway surfaces more uniformly (Kleinstreuer and Zhang, 2010). The particle deposition distribution in the human respiratory system could influence their detrimental effect on human health. For example, it was found that the local accumulation of particles within bronchial airway bifurcations, especially at carinal ridges, may play a crucial role in lung cancer induction (Balásházy et al., 2003). On the other hand, the health impact of PM exposure is closely associated with its chemical compositions (Bell et al., 2007). For example, the study by Franklin et al. (2008) showed that certain chemical species such as Al, sulfate, and Ni, could significantly modify the association between $PM_{2.5}$ (PM with an aerodynamic diameter <2.5 μm) and mortality, and the mass of $PM_{2.5}$ alone may not be a sufficient metric for the risk assessment of PM exposure.

Generally, the sources of aerosol may vary from site to site and are closely associated with the size distributions and chemical compositions of resulting airborne PM (Hwang et al., 2008; Lin et al.,

2005). Outdoor airborne PM measurements have been conducted previously in both Singapore and some other Southeast Asian countries. For example, Betha et al. (2014) conducted an annual sampling of $PM_{2.5}$ aerosols on a building rooftop in Singapore and found the $PM_{2.5}$ concentrations increase during the June 2013 haze episode, mainly due to advection of biomass burning from Sumatra, Indonesia. The temporal evolution of smoke episode in Singapore was investigated by Salinas et al. (2013) to analyze the physical and optical properties of smoke particles in October 2010 and the smoke particle growth due to aging, coagulation and condensation mechanisms was detected over several days. During a peat fire episode in Sumatra, Indonesia, See et al. (2007) conducted a series of ambient air sampling at a rural site, a semirural site, and an urban site to investigate the physical and chemical characteristics of particulate emissions from peat fires. Their source apportionment analysis showed that peat smoke can travel long distances and significantly affect the air quality at locations downwind. The study by Fujii et al. (2015) also characterized $PM_{2.5}$ during the peatland fire seasons in Sumatra, Indonesia based on ground-based and source-dominated sampling. They specifically looked at the key organic compounds of peatland fire aerosols and found levoglucosan was the most abundant compound among in the $PM_{2.5}$ mass. The study by Mustaffa et al. (2014) determined the source apportionment of surfactants in marine aerosols at two selected stations along the Malacca Straits based on the principal component analysis combined with multiple linear regression. The study showed that the surfactants in tropical coastal environments were mainly contributed by sea spray and the anthropogenic sources such as motor vehicles and biomass burning. Khan et al. (2016) conducted the apportionment analysis of $PM_{2.5}$ collected at a semi-urban site in Malaysia and identified five potential sources, i.e. motor vehicle emissions coupled with biomass burning, marine/sulfate aerosol, coal burning, nitrate aerosol, and mineral/road dust. Oanh et al. (2013) compared the $PM_{2.5}$ concentrations among the cases of fixed roadsides, traveling routes in congested urban, and less congested suburban areas of Bangkok. They found that 65-75% of the measurements of roadside $PM_{2.5}$ during dry season exceeded 24 h Thailand ambient air quality

standard of 50 μg m^{-3}. However, most of these studies explored the PM levels at background sites but not the ones at the hotspots in an typical urban environment such as traffic, power plant, and industrial emissions, etc (Stone et al., 2010; Yang et al., 2011), but on ones.

The objectives of this study are to evaluate the specific PM exposure levels related to several major PM emission sources (hotspots) in Singapore which is a tropical city-state and characterized by persistent high temperature and relative humidity (RH) all year long. Bus stops are typical hotspots of PM emission and exposure in Singapore (Velasco and Tan, 2016). The average daily passenger-journeys are 4.4 million out of a population of 5.5 million (LTA, 2015). The areas alongside major highways were also observed to be hotspots with respect to PM pollution (Charron et al., 2007; Harrison et al., 2011). In Singapore, a significant proportion of highways needs to go through residential areas and commercial districts due to limited land space and high population density. Located in the western part of Singapore, the Tuas industrial zone is occupied by various power plants, oil refineries, and waste incineration plants. In this work, we characterized the respective particle number and mass concentrations, particle size distributions, and size-dependent chemical compositions at a bus stop, alongside a high way, and at an industrial site. PMF was then applied to determine the main factors contributing to the particle concentrations at the sites. Existing respiratory deposition models were employed to analyze the deposition distributions of particles and selected non-carcinogenic and carcinogenic elements in the human respiratory system. Health risk assessment was conducted by estimating the hazard quotient (HQ) and excess lifetime cancer risk (ELCR) for the elements.

2 Materials and Methods

2.1 Measurement Sites and Instrumentation

A map view of the sampling sites is shown in Figure 1 in the Supporting Information. The bus stop (lat.=1°18'4"N and long.=103°46'26"E) is along Kent Ridge Crescent Road and located outside of the Lee Kong Chian Natural History Museum of the National University of Singapore (NUS). The number of passing vehicles (trucks, cars, and buses) on both the closer and further lanes was counted manually. The detailed data is summarized in Table S1 in the Supplementary Material. The bus stop is shared by five university shuttle bus services and two public bus services. The traffic flow was generally stable with 0.3 trucks per minute, 4.2 cars per minute, and 0.9 buses per minute. Almost all the passing buses (>95%) on the closer lane experienced a stop-start process at the bus stop. Two sampling stations were set up around 1 m away from the curb and 8 m apart at the two ends (front and back) of the bus stop. Each station includes an aerosol spectrometer (GRIMM model 1.109) which sampled particles at a height of 1.5 m indicative of the human breathing zone. A cascade impactor (Sioutas, SKC Inc) was placed onto the front station to measure particle mass concentrations. The spectrometers measured particle number concentrations in the size range of 0.25 – 32.0 μm. The impactor pumps at has a flow rate of 9 L/min and has five stages, i.e., 0 – 0.25, 0.25 – 0.5, 0.5 – 1, 1 – 2.5, and 2.5 – 10 μm, respectively. The sampling pump of the impactor was calibrated before the field measurements. The highway site (lat.=1°18'14"N and long.=103°46'23"E) is alongside the AYE, a heavily trafficked highway in Singapore and located in the University Town of NUS. The measurement stations are 10 m away to the northeast of the highway and around 200 m apart. 10 m is representative of the distance between some residential buildings and highways in Singapore. The measurement stations are about 2 km away from the west coast. The sampling was conducted on September 15, September 16, September 20, September 23, and September 26 2016, respectively. The industrial site (lat.=1°16'41"N and long.=103°38'10"E) is located in the Tuas

industrial zone. The sampling site is close to the sea in all the directions (east, south, west, and north) with a shortest distance of around 350 m.

Figure 1. A map view of the sampling sites. The red dots denote the sampling sites. A: bus stop; B: highway; C: industry.

2.2 Sample Analysis

2.2.1 Sample preparation

Before the field measurements, the filters of the impactor were equilibrated in a constant temperature (25^{o}C) and humidity (30%) chamber for 48 h. All filters were then weighted using a 3-decimal micrograms weighing balance (Mettler Toledo, Model: XP26). After the sampling, the filters loaded with PM were equilibrated for another 48 h in the chamber followed by the gravimetric analysis. Before the subsequent chemical characterization, the filters were stored at -20 ^{o}C. Blank filters were prepared using the same method and used as a control group.

2.2.2 Metals

The metal (Al, Ba, Ca, Cr, Cu, Fe, K, Mg, Mn, Na, Ni, Pb, Se, Sr, and Zn) concentrations in PM was determined following the extraction procedure used by Betha et al. (2014). Each particle-laden filter was firstly cut into two equal parts with one part being used. The metal contents were microwave extracted using HNO_3, H_2O_2, and HF sequentially, and analyzed using an Inductive Coupled Plasma Mass Spectrometer (ICPMS) (ELAN 6100 PerkinElmer, Inc., MA, U.S.A.). The metal concentrations on blank filters were also extracted and served as controls which were subtracted from the concentrations obtained from the experimental samples to minimize systematic bias.

2.2.3 Inorganic anions

The inorganic anions (Br^-, SO_4^{2-}, Cl^-, and NO^{2-}) were firstly extracted in ultrapure water using supersonic beams under 60°C. The anion concentrations were then measured by a Dionex ICS-3000 ion chromatography (IC) system. The concentrations of the anions on blank filters were also extracted and serve as controls which were subtracted from the concentrations obtained from the experimental samples to minimize systematic bias. Detailed information of quality analysis, control and handling of filter extracts were provided in the Supplementary Material.

2.3 Air Mass Trajectory

Transboundary winds could transport particles emitted by regional hotspots (e.g., biomass fire in Indonesia and sea salts from South China Sea) to Singapore (Khan et al., 2016). Especially, the PM emissions from uncontrolled forest and peat land fires in Indonesia have been a major cause for annual haze episodes in Singapore (Betha et al., 2014). 240 h backward air mass trajectory clusters at a height of 500 m were computed using the Hybrid Single-Particle Lagrangian Integrated Trajectory (HYSPLIT) Model (Stein et al., 2015). The trajectory starting time corresponds to the ending time of the last sampling session of each case and one new trajectory was started every 24 h.

2.4 Respiratory Deposition Modeling

Deposition models of nanoparticles and microparticles are generally different because their deposition mechanisms (i.e. inertial impaction, gravitational sedimentation, and Brownian diffusion) differ (Cheng, 2003; Zamankhan et al., 2006). In line with the existing particle deposition models (Chan et al., 1980; Cheng, 2003; Cohen and Asgharian, 1990; Kim and Fisher, 1999; Kim and Iglesias, 1989; Zamankhan et al., 2006; Zhang et al., 2008), the respiratory system is considered in terms of five stages (Figure 2) (zones): oral (stage 1) and nasal (stage 1) airways, trachea (stage 2), bronchial airways from B1 to B6 (stage 3) and from B7 to B15 (stage 4), and the rest of airways (stage 5) for nanoparticles, while four stages: oral (stage 1) and nasal (stage 1) airways, trachea (stage 2), the bronchial airways from B1 to B19 (stage 3), and the rest of airways (stage 4) for microparticles. The amount of particle deposited in the rest of airways is equal to the difference between the total amount of particles inhaled and the amount of particles depositing on the previous airways. The compiled models and parameters for nanoparticle and microparticle deposition in the human respiratory system are summarized in Table S3 – S5 (Please see the Supplementary Material).

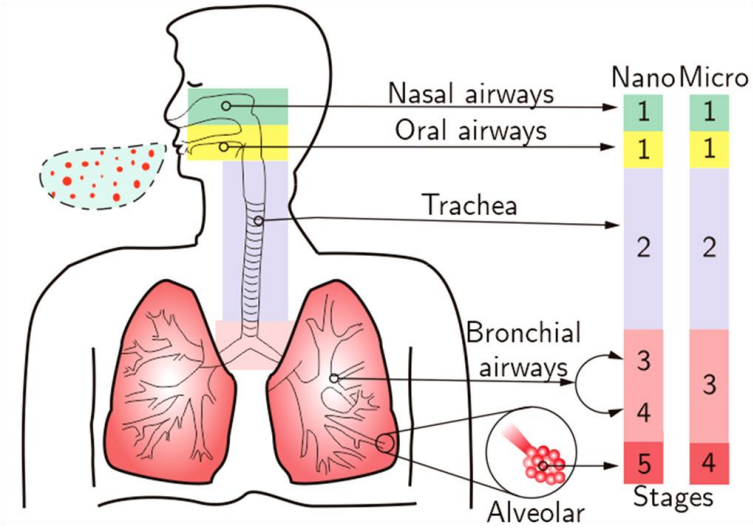

Figure 2. A schematic of the human respiratory system and the arrangements of respiratory stages for nanoparticle and microparticle deposition modeling.

206 The respiratory deposition modeling was conducted with respect to the potential exposure scenarios
207 related to bus stop, highway, and industry. The maximum waiting time for any bus route is around 30
208 min in Singapore, and the interval between the arrival of two consecutive buses is generally within
209 10 min (Velasco and Tan, 2016). Hence, 20-min exposure time was considered for the bus stop
210 scenario. For the highway scenario, we considered residents with houses being alongside highways.
211 In Singapore, the houses are commonly naturally ventilated except during sleeping time and thus
212 have a high particle penetration rate (Balasubramanian and Lee, 2007). The air-conditioners are
213 assumed to be able to filter the outdoor particles during the sleeping time (Batterman et al., 2012). In
214 this scenario, residents coming back from work were assumed to stay indoors for 3 hours before
215 sleep and are subject to the influence of the outdoor aerosol concentration designated by the highway
216 case. For the industry scenario, a case that workers work outdoors for 8 hours per day was
217 considered. The particle mass deposition patterns were computed using the average particle mass
218 concentrations and the average size of each size bin corresponding to the impactor data. The
219 deposition patterns of selected elements (i.e. Cr, Mn, Ni, Pb, and Se) in the respiratory system were
220 also explored. The heavy metals pose a remarkable threat to human health because they could bio-
221 accumulate in the human body (Järup, 2003). Meanwhile, according to International Agency for
222 Research on Cancer (IARC) (IARC, 2017), Cr, Ni and Pb are classified as being carcinogenic to
223 humans, possibly carcinogenic to humans, and probably carcinogenic to humans, respectively.
224

225 ## 2.5 Health Risk Assessment (HRA)

226 The US EPA supplemented guidance (EPA USA, 2009) was applied to estimate the risk of inhalation
227 exposure to the selected elements (i.e. Cr, Mn, Ni, Pb, Se, and Zn) in the three scenarios. The
228 inhalation exposure concentration was estimated by

$$\mathrm{EC}_i = C \times \mathrm{ET} \times \mathrm{EF} \times \mathrm{ED}/\mathrm{ATn} \quad (1)$$

where C (μg/m^3) is the average heavy metal concentration in PM. ET (hours/day), EF (days/year), and ED (years) are the exposure time, frequency, and duration, respectively. ATn is the average time of exposure. For non-carcinogens, ATn = ED × 365 days × 24 hours/day, while for carcinogens, ATn=70 years × 365 days × 24 hours/day.

For the bus stop scenario, ET_b, EF_b, and ED_b are 1/3 hour/day, 300 days/year, and 30 years, respectively. For the highway scenario, HRA is also conducted with respect to residents with houses besides the highway with two sub-scenarios of exposure. In the first sub-scenario, residents coming back from work (EF_{h1}=300 days/year) stay indoors for 3 hours (ET_{h1}=3 hours/day) before sleep. In the second sub-scenario, residents spend another (EF_{h2}=30 days/year) 30 days being at home for the whole day corresponding to ET_{h2} =15 hours/day. The overall risk is the summation of the separate risks of the two sub-scenarios. For the industry scenario, ET_i, EF_i, and ED_i are 8 hours/day, 300 days/year, and 30 years, respectively.

The non-carcinogenic risk is considered by the hazard quotient (HQ) as

$$HQ = EC_i/(RfC \times 1000\ \mu g\ m^{-3}) \quad (2)$$

where RfC (mg·m^{-3}) is the inhalation reference concentration. The cut-off point of significant health risks is HQ=1. The carcinogenic risk is considered by the excess lifetime cancer risk (ELCR) as

$$ELCR = IUR \times EC_i \quad (3)$$

where IUR ((μg m^{-3})$^{-1}$) is the inhalation unit risk. ELCR denotes the probability of developing cancer due to exposure to a specific pollutants for 70 years and its tolerance level is 1×10^{-6}. Both RfC and IUR are obtained from EPA (EPA USA, 2016).

3 Results and Discussion

3.1 Particle Concentrations.

The particle number and volume concentrations of the three cases are given in Table 1. The measured total number concentrations are 179±69, 156±51, and 228±157 #/cm^3 for the cases of bus stop, highway, and industry, respectively. The average number concentration of particles between 0.3 - 10 μm at four different sites (urban, industrial, residential and rural) of Chiang Mai, Thailand was reported to be around 6.8 #/cm^3 (Tippayawong et al., 2006). The smaller number concentration found by Tippayawong et al. (2006) compared to that in this work should be related to the fact that (1) they measured the particles of a narrower size range and (2) their measurements were not directly at the emission hotspots. Khan et al. (2015) observed an average number concentration of particles between 0.25 and 2.5 μm to be 223 #/cm^3 from the measurements on a building rooftop in Selangor, Malaysia. Around 99.9% of the total particle number concentrations are accounted for by particles in the range between 0.25 and 2.5 μm. Khan et al. (2015) found that particles between 0.25 - 0.5 μm contributed to over 99% of the particles between 0.25 - 32 μm via their rooftop measurements in Malaysia. The study by Tippayawong et al. (2006) found that over 90% of the number concentrations of particles between 0.3 - 10 μm at the urban and industrial sites in Chiang Mai, Thailand were accounted for by particles between 0.3 - 1 μm. It is worth noting that the number concentration of $PM_{2.5}$ could reach as high as 1.7× 10^5 cm^{-3} in Indonesia during a peat fire episode (See et al., 2007). The volume concentrations (spherical particles) are estimated to be 10.8±4.0, 11.1±4.8, and 18.0±8.6 μm^3/cm^3, among which particles in the range between 0.25 and 2.5 μm account for 39.2%, 33.8%, and 26.2%, for the cases of bus stop, highway, and industry, respectively. The industry case has 4.93×10^7 - 7.23×10^7 and 3.44×10^4 - 3.69×10^4 #/m^3 higher number of particles than the bus stop and highway cases in the range between 0.25 - 0.65 μm and 2.5 - 32 μm, respectively, while the highway case has 6.01×10^5 and 1.86×10^3 #/m^3 higher number of particles than the bus stop case in the range between 0.5 - 1.0 μm and 5.0 - 32 μm, respectively.

Table 1. Particle (0.25 - 32 μm) number and volume concentrations.

Site	Bus stop	Highway	Industry
Number concentration (#/cm^3)	179 (69)*	156 (51)	228 (157)
Volume concentration (μm^3/cm^3)	10.8 (4.0)	11.1 (4.8)	18.0 (8.6)

*: Values in the brackets are standard deviations.

Figure 3 shows the normalized particle number and volume size distributions. The particle number distributions generally have a single mode, while the particle volume distributions exhibit bimodal features. For the particle diameter larger than 0.4 μm, there are limited differences in the normalized number concentration distributions among the three cases. Tippayawong et al. (2006) also found that the particle number concentrations and size distributions in the range of 0.3-10.0 μm did not exhibit any apparent different between the different sites (urban, industrial, residential and rural) in Chiang Mai, Thailand.

Similar to the study by Khan et al. (2015), the distributions are fitted by the lognormal equation, $y = ae^{-((lnD_p - lnb)/\sqrt{2}lnc)^2}$, where y is the normalized particle number or volume concentrations. D_p is the particle diameter and corresponds to the averages of the size bin edges. a, b, and c are the fitting parameters with b referring to as the count median diameter (CMD) or volume median diameter (VMD), and c as the geometric standard deviation (GSD). For the normalized number concentration distributions, the particle diameter is only shown up to 10 μm (actually, the number concentration of particles larger than 10 μm is negligible) to make the comparison among the three cases more differentiable. The fitting results are listed in Table 2. It is shown that both the CMD and GSD for the number concentration distributions are similar to each other for the three cases. The CMD of this work is larger than while the GSD is smaller than those (around 230 nm for CDM and 1.3 for GSD) found in the study by Khan et al. (2015) which took measurement on a building rooftop. The results suggest that emissions studied in this work have relatively large particle size while the

deviations of particle number concentration across different particle size ranges are relatively small compared with those in the study by Khan et al. (2015). The reason may be these two studies were conducted at different sampling location with different sources of emission. The volume distributions have two VMDs in the accumulation (0.1 - 2 μm) and coarse (>2 μm) mode, respectively. The highway case has the lowest accumulation-mode VMD, suggesting the effect of significant vehicle-related emissions generating relatively small particles. The industry case has a larger coarse-mode VMD than the traffic-related cases. The accumulation- and coarse-mode VMDs of this work are generally larger than the mass median diameter (MMD) (ca. 190 and 2200 nm) reported in the study by Khan et al. (2015). This may be related to the fact that our measurements are closer to the hotspots under an assumption that there are no significant particle density variations across different particle sizes.

Table 2. Results of lognormal fittings against the normalized particle number and volume concentration distributions.

	Fitting parameters	Bus stop	Highway	Industry
Normalized number	CMD (nm)	282.6	279.5	282.3
	GSD	1.10	1.10	1.09
	R^2	0.97	0.98	0.98
Normalized volume	$VMD_{1\#}$ (nm)	273.1	179.8	267.2
	GSD_1	1.34	1.63	1.33
	R_1^2	0.82	0.80	0.80
	VMD_2 (nm)	6039.0	5530.3	8135.6
	GSD_2	2.92	2.34	2.45
	R_2^2	0.70	0.90	0.96

The subscript 1 and 2 denote the fittings with respect to the submicron and micron particles, respectively.
* The values in the bracket denote 95% confidence bounds.

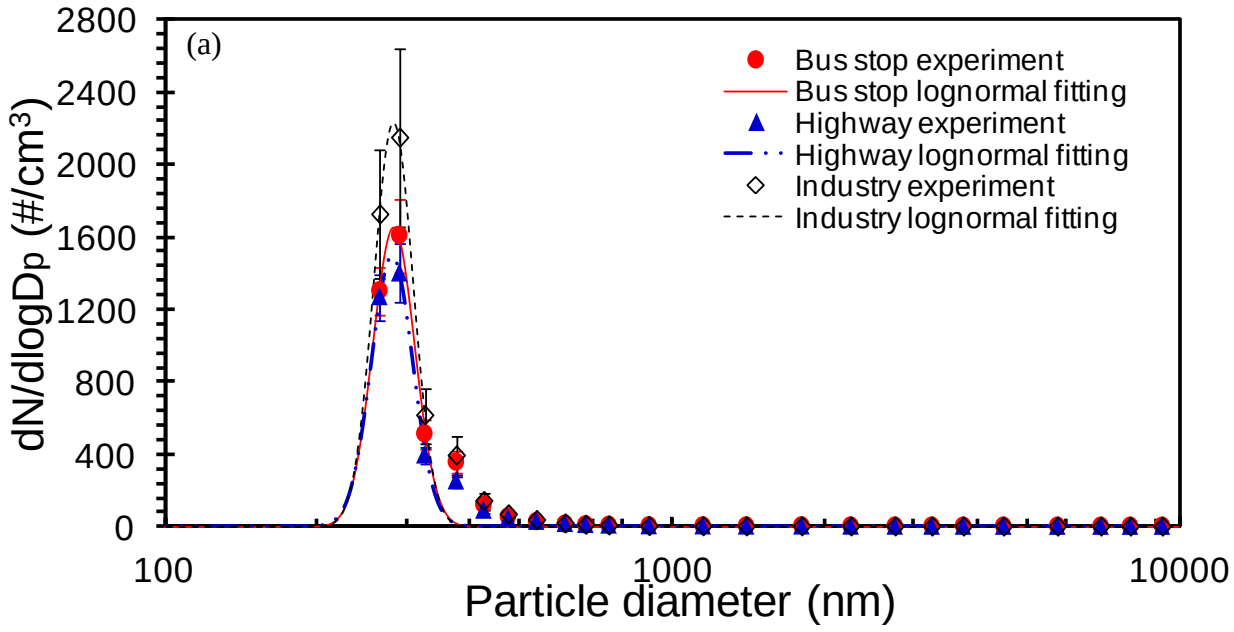

316

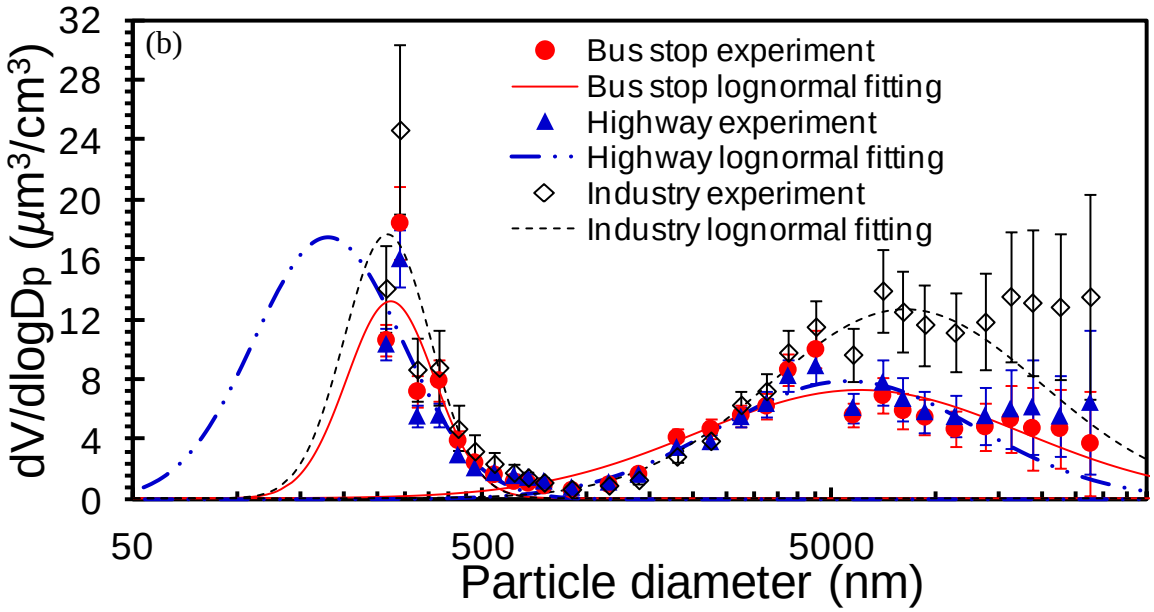

317

318 **Figure 3**. Particle number (a) and volume (b) size distributions with normalized concentrations and
319 corresponding lognormal fittings. Particle sizes correspond to the averages of the size bin edges. The
320 error bars denote one third of the standard deviations.

321

322 The particle mass concentration distributions are shown in Table 3. The traffic-related cases
323 generally have smaller mass concentrations than the industry case in the size range between 0 and
324 0.5 μm, and 1.0 and 10 μm, which is consistent with the data of particle number concentrations
325 (Figure 3). The particle mass concentrations of the bus stop case are generally smaller than that of

the highway case except for particles in the range between 0.25 and 0.5 μm, which is consistent with the data of particle number concentrations as well (Figure 3). This should be related to the fact that the traffic volume on the highway is significantly higher and consisted of by a significant proportion of heavy-duty diesel-powered vehicles (HDDPV), leading to enhanced vehicle-related emissions (Maykut et al., 2003; Morawska et al., 2008). It is worth noting that the mass concentration of particles smaller than 0.25 μm is significantly higher than that of particles between 0.25 and 0.5 μm. This may suggest that there would be significantly high number of particles smaller than 0.25 μm. All the three cases have relatively high mass concentrations in the largest (i.e. 2.5 – 10.0 μm) and smallest (i.e. 0 – 0.25 μm) size bins. The $PM_{2.5}$ and PM_{10} mass concentrations for the industry case are around 30% and 40% higher than the cases of bus stop and highway, respectively. The $PM_{2.5}$ to PM_{10} mass ratio (0.671) for the highway case is larger than that for the bus stop case (0.663), corresponding to the greater fine particle emissions from vehicular sources because of the higher traffic volume of the case of highway. The $PM_{2.5}$ to PM_{10} mass ratio for the industry case is similar to that for the highway case.

Table 3. Particle mass concentration distributions.

Site	Mass concentration[#] ($\mu g/m^3$)				
	0–0.25 μm	0.25–0.5 μm	0.5–1.0 μm	1.0–2.5 μm	2.5–10.0 μm
Bus stop	11.68 (0.16)*	3.79 (0.19)	0.97 (0.18)	2.87 (0.14)	10.27 (0.30)
Highway	14.44 (0.16)	2.04 (0.16)	2.44 (0.25)	4.02 (0.16)	10.93 (0.18)
Industrial site	16.13 (0.16)	5.81 (0.16)	1.65 (0.23)	5.10 (0.18)	13.77 (0.07)

On average, three repeated gravimetric measurements were taken. The precision of the microscale for weighing filters is 0.001mg.

*: Values in the brackets are standard deviations.

3.2 Size-dependent Chemical Compositions

The size-dependent chemical compositions are listed in Table 4. For the case of bus stop, Al, Fe, Na, and Zn are the most abundant inorganic elements in PM. Zn and Fe may be contributed by the non-exhaust sources of vehicular emissions i.e., road-tire interaction and brake wear, respectively. Zn is abundant in tires while Fe is an important brake wear metal (Amato et al., 2011; Councell et al., 2004). As one of major crustal elements (Marcazzan et al., 2003), Fe may have also come from the traffic-induced resuspension of soil dust. The same source may also contribute to Al which has a similar size-dependent concentration distribution to Fe. Both sea-salts and road-salts may have contributed to the Na content in the traffic-related cases (Furusjö et al., 2007).

Similar to the case of bus stop, Al, Fe, Na, and Zn are also the most abundant inorganic elements in PM for the case of highway, in line with the considerable role of vehicular emissions in both of the cases. However, the overall concentrations of these elements in PM_{10} and $PM_{2.5}$ for the highway case are generally higher than that for the bus stop case, which is consistent with the overall higher traffic volume and speed on the highway. For example, although sea-salts may affect the bus stop and highway sites similarly, there should be significantly more road-salts for the highway site in view of the higher traffic volume and speed on the highway, resulting in high Na concentrations in large particles (Beevers and Carslaw, 2005; Thorpe et al., 2007). Moreover, the significant more HDDPV under high-speed cruise phase on the highway may have led to more Na emission in particles smaller than 0.5 μm (Robert et al., 2007). As a result, the Na concentration in PM_{10} and $PM_{2.5}$ of the highway case is about double of that of the bus case. The driving modes of vehicles could affect the size-dependent chemical compositions (Beevers and Carslaw, 2005; Thorpe et al., 2007). For example, the Fe concentration in particles smaller than 0.25 μm for the case of bus stop is significantly higher than that for the case of highway. This should be related to the fact that frequent deceleration and braking events occur at the bus stop giving rise to a significant number of brake

wear particles of the number mode smaller than 0.25 μm and thus increasing the Fe concentration (Vu et al., 2015). The K concentration in PM_{10} and $PM_{2.5}$ for the highway case is about 3 – 4 times of that for the bus stop case, which could potentially be attributed to two aspects. First, the larger number of HDDPV on the highway than the bus stop contributes to more K in particles smaller than 0.5 μm (Dallmann et al., 2014). Second, as an inorganic tracer for biomass burning (Cheng et al., 2013), some of K should have come from the long-distance transport of particles emitted from forest and peat land fires in Sumatra, Indonesia. During the sampling periods at the bus stop and industry sites, the air masses (Figure 4 (a) and (c)) mainly came from java and South China Sea and brought particles emitted from ships and sea spray. On the other hand, during the sampling periods at the highway site, the air masses (Figure 4 (b)) originated from Sumatra (to the southeast of Singapore) brought the particles emitted by the forest and peat land fires (Betha et al., 2014).

Table 4. Size-dependent chemical compositions.

	Bus stop					Highway					Industry				
$C^{\#}$ (ng/m^3)	2.5 - 10 μm	1.0 - 2.5μm	0.5 - 1μm	0.25 - 0.5μm	0 - 0.25 μm	2.5 - 10μm	1.0 - 2.5μm	0.5 - 1μm	0.25 - 0.5μm	0 - 0.25 μm	2.5 - 10 μm	1.0 - 2.5μm	0.5 - 1μm	0.25 - 0.5μm	0 - 0.25 μm
Al	540.67 (17.48)*	312.12 (7.43)	179.46 (3.55)	-**	60.26 (9.50)	1228.99 (28.11)	-	509.57 (12.27)	94.32 (5.22)	261.54 (9.83)	240.53 (8.38)	104.70 (15.27)	-	72.83 (6.45)	122.42 (4.14)
Ba	8.77 (0.26)	5.93 (0.08)	2.79 (0.51)	-	1.90 (0.22)	34.13 (0.67)	5.07 (0.27)	9.76 (0.32)	2.59 (0.49)	5.39 (0.39)	6.27 (0.31)	1.82 (0.41)	-	3.31 (0.03)	3.62 (0.50)
Ca	173.02 (1.93)	73.76 (6.45)	86.22 (3.20)	-	-	513.01 (15.12)	-	191.92 (2.99)	5.43 (3.48)	85.16 (8.53)	62.59 (5.91)	-	-	-	-
Cu	-	-	-	-	--	67.79 (2.01)	-	39.79 (0.47)	-	6.49 (1.05)	-	-	-	-	-
Cr	3.28 (0.26)	5.37 (0.21)	9.13 (0.09)	1.35 (0.09)	31.47 (0.35)	19.88 (0.98)	11.45 (0.14)	22.16 (0.46)	12.56 (0.26)	33.58 (0.12)	6.42 (0.13)	1.46 (0.23)	1.32 (0.17)	1.24 (0.08)	39.78 (0.64)
Fe	177.79 (1.25)	55.06 (1.50)	48.75 (0.88)	-	103.58 (1.22)	825.53 (6.92)	142.50 (0.31)	271 (4.16)	152.19 (2.00)	71.42 (1.07)	533.29 (5.36)	171.42 (2.49)	77.88 (2.06)	168.07 (1.06)	483.96 (8.11)

K	124.06 (0.63)	50.27 (5.11)	14.48 (6.67)	-	36.93 (5.66)	396.43 (17.18)	-	159.32 (5.97)	63.12 (7.99)	154.41 (9.56)	40.03 (3.09)	38.41 (3.22)	1.70 (0.43)	53.95 (8.21)	154.98 (18.63)
Mg	87.92 (4.51)	23.15 (1.77)	8.37 (1.79)	-	29.78 (1.19)	164.65 (4.93)	-	34.36 (2.74)	-	54.60 (1.37)	23.33 (0.50)	-	-	-	7.08 (1.76)
Mn	2.71 (0.17)	0.84 (0.02)	0.87 (0.16)	-	0.74 (0.24)	26.32 (0.57)	1.54 (0.07)	2.87 (0.23)	3.25 (0.43)	4.27 (0.09)	9.55 (0.18)	4.26 (0.26)	0.52 (0.15)	50.93 (0.98)	113.25 (1.67)
Na	765.25 (23.28)	683.05 (25.75)	331.43 (18.89)	-	65.83 (5.43)	1997.10 (78.48)	-	1406.75 (25.06)	240.31 (25.28)	768.46 (39.95)	-	74.95 (12.56)	-	5.81 (1.58)	151.00 (19.46)
Ni	9.33 (0.39)	20.35 (0.49)	25.71 (0.64)	2.43 (0.06)	12.48 (0.11)	9.19 (0.39)	-	14.61 (0.17)	4.21 (0.34)	9.87 (0.39)	11.94 (0.39)	5.43 (0.02)	3.68 (0.27)	2.67 (0.36)	11.25 (0.69)
Pb	10.26 (0.19)	5.38 (0.03)	4.07 (0.02)	1.33 (0.01)	3.09 (0.06)	19.38 (0.04)	1.48 (0.07)	3.75 (0.07)	1.73 (0.05)	5.29 (0.06)	3.65 (0.01)	1.61 (0.07)	-	4.56 (0.03)	9.20 (0.08)
Se	0.35 (0.02)	-	-	-	-	2.03 (0.03)	-	-	-	-	0.58 (0.02)	0.58 (0.07)	-	-	0.58 (0.07)
Sr	0.21 (0.08)	-	-	-	-	3.17 (0.22)	-	0.84 (0.05)	-	-	-	-	-	-	-
Zn	665.76 (8.21)	620.49 (4.94)	476.01 (4.49)	108.24 (2.05)	86.26 (2.83)	716.60 (14.50)	-	110.26 (4.64)	-	316.74 (6.53)	-	20.93 (3.40)	-	163.07 (3.34)	237.36 (6.12)
Br^-	414.13 (18.21)	322.42 (20.22)	393.44 (7.73)	122.83 (4.89)	59.34 (5.23)	619.71 (31.90)	501.22 (17.66)	118.97 (11.21)	357.39 (30.88)	39.02 (2.20)	744.72 (10.09)	328.45 (17.10)	260.50 (8.87)	162.29 (7.11)	68.79 (2.60)
Cl^-	230.43 (11.07)	121.71 (6.88)	120.66 (16.71)	78.38 (5.71)	95.42 (3.93)	181.62 (10.02)	52.91 (3.32)	78.65 (3.89)	79.28 (4.24)	145.17 (7.72)	560.23 (19.31)	71.39 (3.34)	212.10 (11.80)	153.30 (5.54)	48.87 (0.98)
NO_2^-	-	34.09 (3.20)	-	-	33.55 (0.36)	118.49 (4.14)	-	-	-	-	36.37 (0.76)	-	-	51.42 (3.21)	-
SO_4^{2-}	182.19 (3.32)	111.96 (3.97)	91.99 (1.71)	258.13 (7.01)	1229.77 (54.99)	166.62 (17.76)	128.73 (23.90)	109.5 (0.98)	349.39 (9.87)	1465.55 (29.54)	333.39 (13.31)	111.23 (2.23)	91.74 (1.08)	377.41 (8.34)	979.06 (20.16)

[#]: The detection limits for these chemicals are listed in Table S2 of the Supplementary Material.

*: Values in the brackets are standard deviations.

**: denotes not detectable values.

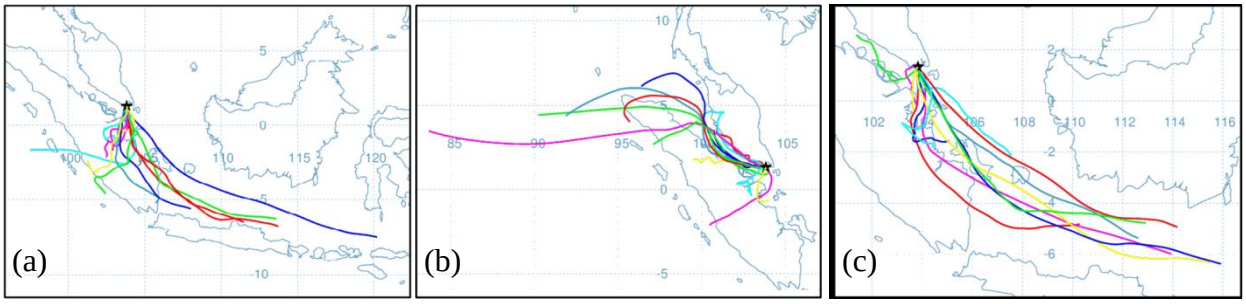

Figure 4. Backward air mass trajectories during the sampling periods of (a) bus stop, (b) highway, and (c) industry computed using the HYSPLIT model.

The Al and Na concentrations in PM_{10} and $PM_{2.5}$ for the industry case are generally smaller than the traffic-related cases, re-emphasizing the close associations between these elements and vehicular sources. However, the Fe concentration for the industry case is similar to the highway case and 50% - 100% higher than the bus stop case. Some steel-related plants in the industrial zone may have contributed to the relatively high Fe concentration. The Zn and Mn concentrations in the particles smaller than 0.5 μm for the industry case are much higher than the traffic-related cases. This suggests the significant emissions of Zn and Mn from some industrial activities such as burning of oil, metallurgical processes, and iron and steel manufacture (Finkelstein and Jerrett, 2007; Marcazzan et al., 2003) in the industrial zone. The Pb concentration in particles smaller than 0.5 μm for the industry case is also higher than that for the traffic-related cases. Several waste incineration plants in the industry zone are potential Pb sources, especially during the treatment of plastic wastes containing lead oxides (Balasubramanian and Qian, 2004). Generally, the metal concentrations obtained in this work are higher than that in the study by Balasubramanian and Qian (2004) which sampled aerosol on a building rooftop in Singapore and thus should better represents the background concentration levels. This re-emphasizes the importance of quantifying the exposure levels near to emission hotspots accessible to people.

409 The cases of bus stop and highway have significantly higher concentrations of SO_4^{2-} than the case of
410 industry in particles smaller than 0.25 μm, suggesting more significant influence of secondary
411 aerosols towards the traffic-related cases. The concentration of SO_4^{2-} in $PM_{2.5}$ for the case of
412 highway is higher than that for the case of bus stop. According to the backward air mass trajectories,
413 as mentioned earlier, the highway case is influenced by the particles emitted from the forest and peat
414 fires in Sumatra (Figure 4) which served as one of the important sources of sulfate for Singapore,
415 especially during haze periods (Balasubramanian et al., 2003). This further confirms the effect of
416 biomass burning in Sumatra on the case of highway. The NO_2^- concentrations in PM_{10} vary from
417 around 70 ng/m^3 (bus stop) to 120 ng/m^3 (highway), which are consistent with the range of
418 particulate NO_2^- levels in urban areas found earlier (NeiláCape, 1996). The particulate NO_2^- is
419 related to the heterogeneous formation of atmospheric HONO onto particle surfaces under high
420 relative humidity conditions (Bigi et al., 2017)., The Cl^- concentrations in both PM_{10} and $PM_{2.5}$ are
421 significantly higher than the Na concentrations for the case of industry, indicating the existence of
422 extra sources in addition to the common ones such as sea-salts and road salts. The waste incineration
423 plants are potential sources because the combustion of solid wastes, especially, plastic materials,
424 could produce significant amount of Cl^- (Vainikka et al., 2011). The concentration of Br^- in $PM_{2.5}$ is
425 the highest for the case of highway followed by the cases of bus stop and industry, respectively.
426 Br^- is an important indicator of vehicular emissions (Chueinta et al., 2000) and thus, compared to the
427 bus stop, the higher traffic volume on the highway emits more Br^-. In the industry zone, the
428 combustion of plastic materials in the waste incineration plants could also serve as a source of
429 Br^- and Br^- has been found in aerosol samples collected from the furnace and electrostatic
430 precipitator ash (Vainikka et al., 2011; Vainikka et al., 2013).
431

3.3 Respiratory Deposition

The particle mass distributions in the human respiratory system are shown in Table 5. Most of the particle mass penetrates deeply into the last stage of the respiratory system, i.e., the 5th and 4th stages for nanoparticles and microparticles, respectively. Particles of 0 - 0.25 μm and 2.5 - 10.0 μm account for around 74%, 74%, and 70% of the particles deposited onto the last stage for the three scenarios, respectively. Significant more nanoparticles deposit onto the first stage for a nasal breathing mode than an oral breathing mode, which indirectly causes 12% more nanoparticles to penetrate deeply to the last stage. Considering that the greatest health concern is related to the deposition of particles into the deep lung system (Cassee et al., 2002; Ferin et al., 1990), the nasal breathing mode serves to mitigate human exposure to aerosols. The breathing mode has insignificant influence on the deposition of microparticles. The daily particle deposition mass to the same respiratory stage is the highest for the industry scenario and is about 4 and 40 times of the scenarios of highway and bus stop, respectively while the particle deposition mass per unit time (i.e., deposition rate) simply corresponds to the airborne particle concentrations as listed in Table 3.

Table 5. A comparison of daily particle mass deposition onto different stages of respiratory system attributed to the exposure related to bus stop, highway, and industry, respectively.

	Particle size (μm)	Stages[&]				
		1	2	3	4	5
Bus stop (ng)	0–0.25	254.3/0*	0.6/0.7	9.1/10.4	4.0/4.6	1835.2/2807.5
	0.25–0.5	82.1/0[†]	0.08/0.09	0.8/0.9	0.4/0.4	599.2/681.1
	0.5–1.0	21.0/0	0/0	0.1/0.1	0.05/0.05	153.5/174.4
	1.0–2.5	0/0	0.4/0.4	0.1/0.1	515.3/515.3	-
	2.5–10.0	0/0	35.5/35.5	55.4/55.4	1758.3/1758.3	-
Highway (ng)	0–0.25	2828.4/0.1	6.5/7.4	101.3/115.2	45.0/51.2	20413.3/23220.5
	0.25–0.5	397.2/0	0.4/0.4	4.0/4.6	1.8/2.0	2899.4/3295.7
	0.5–1.0	473.9/0	0.3/0.3	2.5/2.8	1.1/1.2	3467.2/3940.6
	1.0–2.5	0.2/0	5.4/5.4	1.3/1.3	6506.8/6507.0	-
	2.5–10.0	0.2/0	340.1/340.1	530.1/530.1	16836.0/16836.2	-
Industry (ng)	0–0.25	8422.0/0.3	19.5/22.2	301.6/343.1	134.0/152.4	60783.9/69143.0
	0.25–0.5	3016.8/0	2.8/3.2	30.5/34.7	13.6/15.5	22021.0/25031.4
	0.5–1.0	855.2/0	0.5/0.5	4.4/5.0	2.0/2.2	6256.5/7110.8
	1.0–2.5	0.6/0	18.4/18.4	4.5/4.5	22010.4/22010.9	-
	2.5–10.0	0.8/0	1142.8/1142.8	1780.9/1781.0	56567.1/56567.8	-

*: The values before and after the slash denote the nasal and oral inhalation cases, respectively.

†: The values are rounded to the first decimal place and the small difference of the total deposition mass between the nasal and oral inhalation cases is due to rounding error.

&: Please note the difference in defining the respiratory stages between nanoparticles and microparticles based on the availability of the mathematical models (Figure 3). The stages 3 and 4 for nanoparticles are approximate to the stage 3 for microparticles.

Table 6 lists the daily mass deposition of selected elements onto different stages of the respiratory system attributed to the exposure related to bus stop, highway, and industry, respectively. Corresponding to the mass deposition patterns, most of the mass of the elements also penetrate deeply into the human respiratory system. The highway and industry scenarios correspond to a significant amount of Cr and Ni deposition deep in the lung system per day. It is worth noting that the accumulation of Cr and Ni in lung tumors may contribute to the development of lung cancer (Kuo et al., 2006). The deposition rate of Cr is the highest for the case of highway, which is about double of both the bus stop and industry cases, while the deposition rate of Ni for the case of bus stop is about double of that of highway and industry. The daily deposition rates of Cr and Ni in the lung region were 170 and 220 ng/day, and 55 and 140 ng/day for the highway and industry exposure scenarios, respectively. The industry scenario also corresponds to a significant amount of Mn deposition, with a deposition rate around one order of magnitude higher than that for the cases of bus stop and highway. The industry scenario corresponds to the highest amount of Pb deposition followed by the scenarios of highway and bus stop, respectively, whereas the deposition rate is the highest for the highway case followed by the cases of bus stop and industry, respectively.

Table 6. A comparison of the daily mass deposition of selected elements onto different stages of respiratory system attributed to the exposure related to bus stop, highway, and industry, respectively.

	Element	Stages			
		1	2	3	4
Bus stop	Cr	1.02/0	0.01/0.01	0.06/0.06	8.57/9.58

(ng)	Mn	0.04/0	0/0	0.01/0.01	0.79/0.83
	Ni	0.93/0	0.03/0.03	0.07/0.07	10.97/11.91
	Pb	0.20/0	0.03/0.03	0.05/0.05	3.75/3.95
	Se	0/0	0/0	0/0	0.05/0.05
Highway (ng)	Cr	14.24/0	0.52/0.53	1.24/1.31	163.05/177.22
	Mn	1.99/0	0.63/0.63	1.03/1.04	50.00/51.98
	Ni	5.81/0	0.22/0.23	0.50/0.52	52.99/58.78
	Pb	2.27/0	0.46/0.46	0.79/0.80	43.78/46.04
	Se	0/0	0.05/0.05	0.07/0.07	2.37/2.37
Industry (ng)	Cr	25.75/0	0.52/0.52	1.98/2.16	214.00/239.60
	Mn	99.66/0	0.88/0.90	5.08/5.64	771.38/870.45
	Ni	10.37/0	0.88/0.88	1.71/1.77	137.62/147.94
	Pb	8.32/0	0.28/0.28	0.73/0.78	79.20/87.48
	Se	0.35/0	0.04/0.04	0.08/0.09	6.79/7.15

*: The values before and after the slash denote the nasal and oral inhalation cases, respectively.

†: The values are rounded to the second decimal place and the small difference of the total deposition mass between the nasal and oral inhalation cases is due to rounding error.

3.4 HRA

The HRA results are listed in Table 7. The HRA results show that most of the elements have the non-carcinogenic and carcinogenic risks being within the accepted limits (HQ=1 and ELCR=1×10^{-6}). Generally, the industry exposure scenario has the highest health risk followed by the highway and bus stop scenarios, respectively. Cr poses a potential carcinogenic risk in all the scenarios with the ELCR ranging from 2.1×10^{-5} to 9.8×10^{-4}. The major sources of Cr include industrial emissions (e.g., tanning processes), petroleum refining related fuel combustion, and vehicular sources (Sabin and Schiff, 2008) which should be focused during the design and implementation of effective Cr control measures. The non-carcinogenic risk of Mn in the industry scenario is approaching the acceptable limit because the existence of various significant emission sources (burning of oil, metallurgical factories, iron and steel manufacture, and traffic sources) (Abbott, 1987; Finkelstein and Jerrett, 2007) in the industrial zone. Both Ni and Mn may pose a potential non-carcinogenic risk for people who are involved with all the three exposure scenarios (i.e. people who commute by public transport and work in the industrial zone with home alongside highways) in addition to the carcinogenic risk by Cr.

And the risk is mainly accounted for by the highway and industry exposure. Measures such as applying air purifiers at homes and reducing the penetration of outdoor particles by closing windows may serve to mitigate the human inhalation exposure to the particles.

Table 7. Health risks for the inhalation exposure to the selected elements attributed to bus stop, highway, and industry, respectively.

	Bus stop		Highway		Industry	
	HQ*	ELCR*	HQ	ELCR	HQ	ELCR
Cr	5.8×10^{-3}	2.1×10^{-5}	1.5×10^{-1}	5.6×10^{-4}	1.4×10^{-1}	9.8×10^{-4}
Mn	1.2×10^{-3}	-	1.2×10^{-1}	-	9.8×10^{-1}	-
Ni	5.7×10^{-2}	8.3×10^{-8}	4.2×10^{-1}	6.0×10^{-7}	6.8×10^{-1}	1.1×10^{-6}
Pb	1.4×10^{-3}	1.4×10^{-9}	2.4×10^{-2}	2.5×10^{-8}	2.6×10^{-2}	4.5×10^{-8}
Se	2.0×10^{-7}	-	1.6×10^{-5}	-	2.4×10^{-5}	-

* The acceptable risk limits for HQ and ELCR are 1 and 1×10^{-6}, respectively.

4 Conclusions

In this work, we evaluate the particulate exposure related to several emission hotspots, i.e., bus stop, highway, and industry in a hot and humid tropical city, Singapore. The industry case had higher number of particles than the bus stop and highway cases in the range between 0.25 and 0.65 μm and 2.5 and 32 μm, respectively, while the highway case had higher number of particles than the bus stop case in the range between 0.5 and 1.0 μm and 5.0 and 32 μm, respectively. The $PM_{2.5}$ and PM_{10} mass concentrations for the industry case are around 30% and 40% higher than the cases of bus stop and highway, respectively. Al, Fe, Na, and Zn are the most abundant inorganic elements in PM for the traffic-related cases, while Zn, Mn, Fe, and Pb are abundant for the industry case. The respiratory deposition modeling shows that particles of 0 - 0.25 μm and 2.5 - 10.0 μm account for around 74%, 74%, and 70% of the particles deposited onto the last stages of the respiratory system. The deposition rate of Cr is the highest for the case of highway, which is about double of the cases of bus stop and industry, while the deposition rate of Ni for the case of bus stop is about double of that of highway and industry. The industry scenario also corresponds to a significant amount of Mn deposition, with a deposition rate around one order of magnitude higher than that for the cases of bus stop and

highway. Health risk assessment shows that Cr poses a potential carcinogenic risk in all the scenarios. Both Ni and Mn may pose a potential non-carcinogenic risk for people who are involved with all the three exposure scenarios.

Acknowledgement

This research program is funded by the National Research Foundation (NRF), Prime Minister's Office, Singapore under its Campus for Research Excellence and Technological Enterprise (CREATE) program.

Appendix A. Supplementary Material

Additional Data could be found in the Supplementary Material.

REFERENCES

Abbott, P.J. Methylcyclopentadienyl manganese tricarbonyl (MMT) in petrol: the toxicological issues. Sci. Total Environ. 1987;67:247-255.

Amato, F.; Viana, M.; Richard, A.; Furger, M.; Prévôt, A.; Nava, S.; Lucarelli, F.; Bukowiecki, N.; Alastuey, A.; Reche, C. Size and time-resolved roadside enrichment of atmospheric particulate pollutants. Atmos. Chem. Phys. 2011;11:2917-2931.

Atkinson, R.W.; Ross Anderson, H.; Sunyer, J.; Ayres, J.; Baccini, M.; Vonk, J.M.; Boumghar, A.; Forastiere, F.; Forsberg, B.; Touloumi, G. Acute effects of particulate air pollution on respiratory admissions: results from APHEA 2 project. Am. J. Resp. Crit. Care Med. 2001;164:1860-1866.

Balásházy, I.; Hofmann, W.; Heistracher, T. Local particle deposition patterns may play a key role in the development of lung cancer. J. Appl. Physiol. 2003;94:1719-1725.

Balasubramanian, R.; Lee, S.S. Characteristics of indoor aerosols in residential homes in urban locations: a case study in Singapore. J. Air Waste Manag. Assoc. 2007;57:981-990.

Balasubramanian, R.; Qian, W. Characterization and source identification of airborne trace metals in Singapore. J. Environ. Monit. 2004;6:813-818.

Balasubramanian, R.; Qian, W.B.; Decesari, S.; Facchini, M.; Fuzzi, S. Comprehensive characterization of $PM_{2.5}$ aerosols in Singapore. J. Geophys Res. 2003;108

Batterman, S.; Du, L.; Mentz, G.; Mukherjee, B.; Parker, E.; Godwin, C.; Chin, J.Y.; O'toole, A.; Robins, T.; Rowe, Z. Particulate matter concentrations in residences: an intervention study evaluating stand-alone filters and air conditioners. Indoor Air 2012;22:235-252.

Beevers, S.D.; Carslaw, D.C. The impact of congestion charging on vehicle emissions in London. Atmos. Environ. 2005;39:1-5.

Bell, M.L.; Dominici, F.; Ebisu, K.; Zeger, S.L.; Samet, J.M. Spatial and temporal variation in $PM_{2.5}$ chemical composition in the United States for health effects studies. Environ. Health Perspect. 2007:989-995.

Betha, R.; Behera, S.N.; Balasubramanian, R. 2013 Southeast Asian smoke haze: fractionation of particulate-bound elements and associated health risk. Environ. Sci. Technol. 2014;48:4327-4335.

Bigi, A.; Bianchi, F.; De Gennaro, G.; Di Gilio, A.; Fermo, P.; Ghermandi, G.; Prévôt, A.; Urbani, M.; Valli, G.; Vecchi, R. Hourly composition of gas and particle phase pollutants at a central urban background site in Milan, Italy. Atmos. Res. 2017;186:83-94.

Cassee, F.R.; Muijser, H.; Duistermaat, E.; Freijer, J.J.; Geerse, K.B.; Marijnissen, J.C.; Arts, J.H. Particle size-dependent total mass deposition in lungs determines inhalation toxicity of cadmium chloride aerosols in rats. Application of a multiple path dosimetry model. Arch. Toxicol. 2002;76:277-286.

Chan, T.L.; Schreck, R.M.; Lippmann, M. Effect of the laryngeal jet on particle deposition in the human trachea and upper bronchial airways. J. Aerosol Sci. 1980;11:447-459.

Charron, A.; Harrison, R.M.; Quincey, P. What are the sources and conditions responsible for exceedences of the 24h PM_{10} limit value ($50\mu gm^{-3}$) at a heavily trafficked London site? Atmos. Environ. 2007;41:1960-1975.

Cheng, Y.; Engling, G.; He, K.-B.; Duan, F.-K.; Ma, Y.-L.; Du, Z.-Y.; Liu, J.-M.; Zheng, M.; Weber, R.J. Biomass burning contribution to Beijing aerosol. Atmos. Chem. Phys. 2013;13:7765-7781.

Cheng, Y.S. Aerosol deposition in the extrathoracic region. Aerosol Sci. Technol. 2003;37:659-671.

Chueinta, W.; Hopke, P.K.; Paatero, P. Investigation of sources of atmospheric aerosol at urban and suburban residential areas in Thailand by positive matrix factorization. Atmos. Environ. 2000;34:3319-3329.

Cohen, B.; Asgharian, B. Deposition of ultrafine particles in the upper airways: an empirical analysis. J. Aerosol Sci. 1990;21:789-797.

577 Councell, T.B.; Duckenfield, K.U.; Landa, E.R.; Callender, E. Tire-wear particles as a source of zinc
578 to the environment. Environ. Sci. Technol. 2004;38:4206-4214.
579 Dallmann, T.R.; Onasch, T.B.; Kirchstetter, T.W.; Worton, D.R.; Fortner, E.; Herndon, S.; Wood, E.;
580 Franklin, J.; Worsnop, D.; Goldstein, A. Characterization of particulate matter emissions
581 from on-road gasoline and diesel vehicles using a soot particle aerosol mass spectrometer.
582 Atmos. Chem. Phys. 2014;14:7585-7599.
583 Donaldson, K.; Stone, V.; Seaton, A.; MacNee, W. Ambient particle inhalation and the
584 cardiovascular system: potential mechanisms. Environ. Health Perspect. 2001;109:523.
585 EPA USA. Risk Assessment Guidance for Superfund Volume I: Human Health Evaluation Manual
586 (Part F, Supplemental Guidance for Inhalation Risk Assessment):
587 https://www.epa.gov/risk/risk-assessment-guidance-superfund-rags-part-f; [accessed at
588 Dec/19/2016].
589 EPA USA. Regional Screening Levels (RSLs) - Generic Tables (May 2016):
590 https://www.epa.gov/risk/regional-screening-levels-rsls-generic-tables-may-2016; [accessed
591 at Dec/19/2016].
592 Ferin, J.; Oberdörster, G.; Penney, D.; Soderholm, S.; Gelein, R.; Piper, H. Increased pulmonary
593 toxicity of ultrafine particles? I. Particle clearance, translocation, morphology. J. Aerosol Sci.
594 1990;21:381-384.
595 Finkelstein, M.M.; Jerrett, M. A study of the relationships between Parkinson's disease and markers
596 of traffic-derived and environmental manganese air pollution in two Canadian cities. Environ.
597 Res. 2007;104:420-432.
598 Franklin, M.; Koutrakis, P.; Schwartz, J. The role of particle composition on the association between
599 $PM_{2.5}$ and mortality. Epidemiology 2008;19:680.
600 Fujii, Y.; Kawamoto, H.; Tohno, S.; Oda, M.; Iriana, W.; Lestari, P. Characteristics of carbonaceous
601 aerosols emitted from peatland fire in Riau, Sumatra, Indonesia (2): identification of organic
602 compounds. Atmos. Environ. 2015;110:1-7.
603 Furusjö, E.; Sternbeck, J.; Cousins, A.P. PM_{10} source characterization at urban and highway roadside
604 locations. Sci. Total Environ. 2007;387:206-219.
605 Harrison, R.M.; Beddows, D.C.; Dall'Osto, M. PMF analysis of wide-range particle size spectra
606 collected on a major highway. Environ. Sci. Technol. 2011;45:5522-5528.
607 Hwang, I.; Hopke, P.K.; Pinto, J.P. Source apportionment and spatial distributions of coarse particles
608 during the regional air pollution study. Environ. Sci. Technol. 2008;42:3524-3530.

609 IARC, International Agency for Research on Cancer. IARC monographs on the evaluation of
610 carcinogenic risks to humans: http://monographs.iarc.fr/ENG/Classification/; [Accessed at
611 Dec/19/2016].
612 Järup, L. Hazards of heavy metal contamination. Br. Med. Bull. 2003;68:167-182.
613 Khan, M.; Latif, M.T.; Saw, W.; Amil, N.; Nadzir, M.; Sahani, M.; Tahir, N.; Chung, J. Fine
614 particulate matter in the tropical environment: monsoonal effects, source apportionment, and
615 health risk assessment. Atmos. Chem. Phys. 2016;16:597-617.
616 Khan, M.F.; Latif, M.T.; Amil, N.; Juneng, L.; Mohamad, N.; Nadzir, M.S.M.; Hoque, H.M.S.
617 Characterization and source apportionment of particle number concentration at a semi-urban
618 tropical environment. Environ. Sci. Pollut. Res. 2015;22:13111-13126.
619 Kim, C.S.; Fisher, D.M. Deposition characteristics of aerosol particles in sequentially bifurcating
620 airway models. Aerosol Sci. Technol. 1999;31:198-220.
621 Kim, C.S.; Iglesias, A.J. Deposition of inhaled particles in bifurcating airway models: I. Inspiratory
622 deposition. J. Aerosol Med. 1989;2:1-14.
623 Kleinstreuer, C.; Zhang, Z. Airflow and particle transport in the human respiratory system. Annu.
624 Rev. Fluid Mech. 2010;42:301-334.
625 Kuo, C.-Y.; Wong, R.-H.; Lin, J.-Y.; Lai, J.-C.; Lee, H. Accumulation of chromium and nickel
626 metals in lung tumors from lung cancer patients in Taiwan. J. Toxicol. Environ. Health Part
627 A 2006;69:1337-1344.
628 Liao, D.; Creason, J.; Shy, C.; Williams, R.; Watts, R.; Zweidinger, R. Daily variation of particulate
629 air pollution and poor cardiac autonomic control in the elderly. Environ. Health Perspect.
630 1999;107:521.
631 Lin, C.-C.; Chen, S.-J.; Huang, K.-L.; Hwang, W.-I.; Chang-Chien, G.-P.; Lin, W.-Y. Characteristics
632 of metals in nano/ultrafine/fine/coarse particles collected beside a heavily trafficked road.
633 Environ. Sci. Technol. 2005;39:8113-8122.
634 LTA. Singapore Land Transport: Statistics In Brief 2015. Land Transport Authority, Singapore. .
635 2015: https://www.lta.gov.sg/content/ltaweb/en/publications-and-research.html; [accessed at
636 Dec/1/2016].
637 Marcazzan, G.; Ceriani, M.; Valli, G.; Vecchi, R. Source apportionment of PM_{10} and $PM_{2.5}$ in Milan
638 (Italy) using receptor modelling. Sci. Total Environ. 2003;317:137-147.
639 Maykut, N.N.; Lewtas, J.; Kim, E.; Larson, T.V. Source apportionment of $PM_{2.5}$ at an urban
640 IMPROVE site in Seattle, Washington. Environ. Sci. Technol. 2003;37:5135-5142.

641 Morawska, L.; Ristovski, Z.; Jayaratne, E.; Keogh, D.U.; Ling, X. Ambient nano and ultrafine
642 particles from motor vehicle emissions: Characteristics, ambient processing and implications
643 on human exposure. Atmos. Environ. 2008;42:8113-8138.
644 Mustaffa, N.I.H.; Latif, M.T.; Ali, M.M.; Khan, M.F. Source apportionment of surfactants in marine
645 aerosols at different locations along the Malacca Straits. Environ. Sci. Pollut. Res.
646 2014;21:6590-6602.
647 NeiláCape, J. Nitrous acid and nitrite in the atmosphere. Chem. Soc. Rev. 1996;25:361-369.
648 Nel, A. Air pollution-related illness: effects of particles. Science 2005;308:804-806.
649 Norris, G.; YoungPong, S.N.; Koenig, J.Q.; Larson, T.V.; Sheppard, L.; Stout, J.W. An association
650 between fine particles and asthma emergency department visits for children in Seattle.
651 Environ. Health Perspect. 1999;107:489.
652 Oanh, N.K.; Kongpran, J.; Hang, N.; Parkpian, P.; Hung, N.; Lee, S.-B.; Bae, G.-N. Characterization
653 of gaseous pollutants and $PM_{2.5}$ at fixed roadsides and along vehicle traveling routes in
654 Bangkok Metropolitan Region. Atmos. Environ. 2013;77:674-685.
655 Robert, M.A.; Kleeman, M.J.; Jakober, C.A. Size and composition distributions of particulate matter
656 emissions: Part 2-Heavy-duty diesel vehicles. J. Air Waste Manag. Assoc. 2007;57:1429-
657 1438.
658 Sabin, L.D.; Schiff, K.C. Dry atmospheric deposition rates of metals along a coastal transect in
659 southern California. Atmos. Environ. 2008;42:6606-6613.
660 Salinas, S.V.; Chew, B.N.; Miettinen, J.; Campbell, J.R.; Welton, E.J.; Reid, J.S.; Liya, E.Y.; Liew,
661 S.C. Physical and optical characteristics of the October 2010 haze event over Singapore: A
662 photometric and lidar analysis. Atmos. Res. 2013;122:555-570.
663 See, S.W.; Balasubramanian, R.; Rianawati, E.; Karthikeyan, S.; Streets, D.G. Characterization and
664 source apportionment of particulate matter$\leqslant$2.5 μm in Sumatra, Indonesia, during a recent
665 peat fire episode. Environ. Sci. Technol. 2007;41:3488-3494.
666 Stein, A.; Draxler, R.; Rolph, G.; Stunder, B.; Cohen, M.; Ngan, F. NOAA's HYSPLIT atmospheric
667 transport and dispersion modeling system. B. Am. Meteorol. Soc. 2015;96:2059-2077.
668 Stone, E.; Schauer, J.; Quraishi, T.A.; Mahmood, A. Chemical characterization and source
669 apportionment of fine and coarse particulate matter in Lahore, Pakistan. Atmos. Environ.
670 2010;44:1062-1070.
671 Tecer, L.H.; Alagha, O.; Karaca, F.; Tuncel, G.; Eldes, N. Particulate matter ($PM_{2.5}$, $PM_{10\text{-}2.5}$, and
672 PM_{10}) and children's hospital admissions for asthma and respiratory diseases: A bidirectional
673 case-crossover study. J. Tox. Env. Health. 2008;71:512-520.

674 Thorpe, A.J.; Harrison, R.M.; Boulter, P.G.; McCrae, I.S. Estimation of particle resuspension source
675 strength on a major London Road. Atmos. Environ. 2007;41:8007-8020.
676 Tippayawong, N.; Pengchai, P.; Lee, A. Characterization of ambient aerosols in Northern Thailand
677 and their probable sources. Int. J. Environ. Sci. Technol. 2006;3:359-369.
678 Turner, M.C.; Krewski, D.; Pope III, C.A.; Chen, Y.; Gapstur, S.M.; Thun, M.J. Long-term ambient
679 fine particulate matter air pollution and lung cancer in a large cohort of never-smokers. Am. J.
680 Resp. Crit. Care Med. 2011;184:1374-1381.
681 Vainikka, P.; Enestam, S.; Silvennoinen, J.; Taipale, R.; Yrjas, P.; Frantsi, A.; Hannula, J.; Hupa, M.
682 Bromine as an ash forming element in a fluidised bed boiler combusting solid recovered fuel.
683 Fuel 2011;90:1101-1112.
684 Vainikka, P.; Lindberg, D.; Moilanen, A.; Ollila, H.; Tiainen, M.; Silvennoinen, J.; Hupa, M. Trace
685 elements found in the fuel and in-furnace fine particles collected from 80MW BFB
686 combusting solid recovered fuel. Fuel Process. Technol. 2013;105:202-211.
687 Velasco, E.; Tan, S.H. Particles exposure while sitting at bus stops of hot and humid Singapore.
688 Atmos. Environ. 2016;142:251-263.
689 Vu, T.V.; Delgado-Saborit, J.M.; Harrison, R.M. Review: Particle number size distributions from
690 seven major sources and implications for source apportionment studies. Atmos. Environ.
691 2015;122:114-132.
692 Yang, F.; Tan, J.; Zhao, Q.; Du, Z.; He, K.; Ma, Y.; Duan, F.; Chen, G. Characteristics of $PM_{2.5}$
693 speciation in representative megacities and across China. Atmos. Chem. Phys. 2011;11:5207-
694 5219.
695 You, S.; Tong, Y.W.; Neoh, K.G.; Dai, Y.; Wang, C.-H. On the association between outdoor $PM_{2.5}$
696 concentration and the seasonality of tuberculosis for Beijing and Hong Kong. Environ. Pollut.
697 2016;218:1170-1179.
698 Zamankhan, P.; Ahmadi, G.; Wang, Z.; Hopke, P.K.; Cheng, Y.-S.; Su, W.C.; Leonard, D. Airflow
699 and deposition of nano-particles in a human nasal cavity. Aerosol Sci. Technol. 2006;40:463-
700 476.
701 Zhang, Z.; Kleinstreuer, C.; Kim, C.S. Airflow and nanoparticle deposition in a 16-generation
702 tracheobronchial airway model. Ann. Biomed. Eng. 2008;36:2095-2110.